Iron(II) Complexes Containing a Ferrocenyl Framework Attached to 2,2′-bipyridine or 1,10-phenanthroline Subunits: Formation of Stable Fe-bis(2,2′-bipyridine)-like and Fe-bis(1,10-phenanthroline)-like Complexes

Ana Ion,[‡,#] Jean-Claude Moutet,*[,‡] Eric Saint-Aman,[‡] Guy Royal,[‡] Sophie Tingry,[‡] Jacques Pecaut,[⊥] Stephane Menage,[+] and Raymond Ziessel[¶]

Laboratoire d'Electrochimie Organique et de Photochimie Rédox, UMR CNRS 5630, Université Joseph Fourier Grenoble I, BP 53, 38041 Grenoble Cédex 9, France, DRFMC|CEA|SCIB, Laboratoire de Chimie de Coordination, 17 rue des Martyrs, 38054 Grenoble Cédex 9, France, Laboratoire de Chimie et Biochimie des Centres Rédox biologiques, Université Joseph Fourier, DBMS|CEA, EP CNRS 1087, 17 rue des Martyrs, 38054 Grenoble Cédex 9, France, and Laboratoire de Chimie, d'Electronique et de Photonique Moléculaires, Ecole de Chimie, Matériaux, Polymères, Université Louis-Pasteur, ECPM UPRES-A 7008, 1 rue Blaise Pascal, BP 296 F, 67008 Strasbourg Cédex, France

Received August 1, 2000

Introduction

Coordination of iron(II) with 2,2′-bipyridine (bipy) and 1,10-phenanthroline (phen) ligands leads generally to highly stable tris-bipy or phen complexes. Complexes of the type $[Fe^{II}(\mathbf{L})_2X_2]$ containing only two such ligands have been obtained with anionic ligands (**L** = bipy, phen; X = CN^-, SCN^-, Cl^-, for example).[1] Very recently, $[Fe^{II}(\mathbf{L})_2S_2]^{2+}$ species with two open sites filled by solvent molecules (S = H_2O or CH_3CN) have been characterized in solution on the basis of electrochemical and UV−vis data.[2,3] However, their poor stability precluded any further characterization by mass spectrometry and/or solid-state X-ray structure analysis.

Apart from our ongoing interest in redox-active polypyridyl ligands that are able to electrochemically recognize transition metal complexes in homogeneous solution[4] and in polymer films,[5] we report here the coordination of Fe^{2+} with 1-bipy, 1,1′-bis(bipy), and 1,1′-bis(phen) carboxamide or carboxyester-bridged derivatives of ferrocene, sketched in Chart 1 as ligands $\mathbf{L}^{1-3}$. The unprecedented formation of stable complexes where the iron (II) environment is provided by the four nitrogen atoms of the bipy or phen subunits and by the two oxygen atoms of the carbonyl groups belonging to the amide or ester linkages is described. This unexpected coordination mode is evidenced from electrochemical, FT-IR, and UV−visible studies, while the cis arrangement of the carbonyl moieties is confirmed with the help of crystal structures for $[Fe\mathbf{L}^2]^{2+}$ and $[Fe\mathbf{L}^3]^{2+}$ complexes.

Interest in such dinuclear complexes is also stimulated by the study of electronic coupling of both metal centers in different oxidation states and by the coupling of redox active metal centers to potential catalytic sites. Indeed, it is well documented that Fe(II)-bipy complexes catalyze the thermal water oxidation to dioxygen,[6] alkene oxidation with dioxygen,[7] and alkane oxidation with hydroperoxide,[2] but with restricted turnover numbers. It was claimed[6] that "$Fe(bipy)_2$" was the active catalytic species, and that the instability of the system was due to decoordination of a bipy and its subsequent reaction with "$Fe(bipy)_2$" to form the inactive "$Fe(bipy)_3$" species.[2,7] Here we describe tweezer ligands which provide stable Fe-bis(bipy) complexes suspected to behave as redox catalysts.

Experimental Section

Ligands. $\mathbf{L}^1$ and $\mathbf{L}^2$ were synthesized as reported previously.[8] $\mathbf{L}^3$ was prepared by the stoichiometric reaction of 6-(hydroxymethyl)-6′-methyl-1,10-phenanthroline[9] with 1 mmol of 1,1′-bis(chlorocarbonyl)-ferrocene[10] in 10 mL of dried toluene containing 4 mmol of freshly distilled triethylamine. The reaction mixture was stirred overnight, at room temperature under an inert atmosphere, then filtered and evaporated to dryness. The crude product was extracted with CH_2Cl_2, and the organic phase was washed with H_2O. The solvent was removed in vacuo, and the crude product was purified by neutral alumina column chromatography, eluting with CH_2Cl_2 to yield $\mathbf{L}^3$ (79%) as an orange solid. ^{1}H NMR (250 MHz, CD_2Cl_2) δ : 2.76 (s, 6H, C*H*$_3$), 4.52 (m, 4H, *H*-Cp$_{\beta,\beta'}$) ,4.91 (m, 4H, *H*-Cp$_{\alpha,\alpha'}$), 5.52 (s, 4H, C*H*$_2$), 7.50 (d, 2H, *H*-phen), 7.56−7.83 (m, 6H, *H*-phen), 8.14 (d, 2H, *H*-phen), 8.25 (d, 2H, *H*-phen). FAB-MS, *m*/*z*: 687 (M + H^+). UV−vis (d−d band; CH_3CN) λ_{max} (ϵ/M^{-1} cm^{-1}) = 450 nm (300). FT-IR: ν_{CO} = 1713 cm^{-1}. Anal. Calcd for $C_{40}H_{30}N_4O_4Fe$: C, 69.98; H, 4.40; N 8.16. Found: C, 69.26; H, 4.89; N, 8.36.

Complexes. Synthesis of iron complexes as their perchlorate salts was performed by reaction at room temperature in CH_2Cl_2 of stoichiometric amounts of $\mathbf{L}^1$ ($2\mathbf{L}^1$ + 1 Fe), $\mathbf{L}^2$ or $\mathbf{L}^3$ (**L** + 1 Fe) and $Fe(ClO_4)_2 \cdot 6H_2O$. Precipitation was induced by the addition of diethyl oxide, and the products were collected as orange solids by suction filtration. **Warning!** ***Perchlorate salts are hazardous because of the possibility of explosion***. X-ray quality crystals were obtained by vapor diffusion of diethyl ether into an acetonitrile/dichloromethane solution of the complexes.

$[Fe\mathbf{L}^1{}_2](ClO_4)_2$. Yield, 90%. ES$^+$-MS, *m*/*z*: 949 ($[Fe\mathbf{L}^1{}_2](ClO_4)^+$; 49%), 551 ($[Fe\mathbf{L}^1](ClO_4)^+$; 39%), 425 ($[Fe\mathbf{L}^1{}_2]^{2+}$; 100%), 398 ($\mathbf{L}^1$ + H^+; 14%). UV−vis (LMCT band; CH_3CN) λ_{max} (ϵ/M^{-1} cm^{-1}) = 450 nm (610). FT-IR: ν_{CO} = 1633 cm^{-1}. ^{1}H NMR (300 MHz, CD_3CN, 10 mM, 295 K) δ: 69.6 (4H, *H*-*o*-bipy or N*H*), 60.1, 58.2, 56.1 (4H, 2H

* To whom correspondence should be addressed. Fax: (33) 04 76 51 42 67. E-mail: Jean-Claude.Moutet@ujf-grenoble.fr.
‡ Laboratoire d'Electrochimie Organique et de Photochimie Rédox.
⊥ DRFMC|CEA|SCIB, Laboratoire de Chimie de Coordination.
+ Laboratoire de Chimie et Biochimie des Centres Rédox biologiques.
¶ Laboratoire de Chimie, d'Electronique et de Photonique Moléculaires, Université Louis-Pasteur.
# Permanent address: Department of Applied Physical Chemistry and Electrochemistry, Politehnica University, Bucharest, Romania

(1) Hawker, P. N.; Twigg, M. V. In *Comprehensive Coordination Chemistry*; Wilkinson, G., Gillard, R. D., McCleverty, J. A., Eds; Pergamon Press: Oxford, 1987; Vol. 4.
(2) Collomb, M.-N.; Deronzier, A.; Duboc Toia, C.; Fontecave, M.; Gorgy, K.; Leprêtre, J.-C.; Ménage, S. *J. Electroanal. Chem*. **1999**, *469*, 53.
(3) Collomb, M.-N.; Deronzier, A.; Gorgy, K.; Leprêtre, J.-C. *New J. Chem*. **2000**, *24*, 455.
(4) Buda, M.; Moutet, J.-C.; Saint-Aman, E.; De Cian, A.; Fischer, J.; Ziessel, R. *Inorg. Chem.* **1998**, *37*, 4146.
(5) Buda, M.; Moutet, J.-C.; Pailleret, A.; E. Saint-Aman, E.; Ziessel, R. *J. Electroanal. Chem*. **2000**, *484*, 164.
(6) Collin, J.-P.; Lehn, J.-M.; Ziessel, R. *Nouv. J. Chem*. **1982**, *6*, 405.
(7) Hage, J. P.; Powell, J. A.; Sawyer, T. *J. Am. Chem. Soc*. **1995**, *117*, 12897.
(8) Buda, M.; Ion, A.: Moutet, J.-C.; E. Saint-Aman, E.; Ziessel, R. *J. Electroanal. Chem*. **1999**, *469*, 132.
(9) Adapted from: Newkome, G. R.; Theriot, K. J.; Gupta, V. K.; Franczek, F. R.; Bocker, G. R. *J. Org. Chem.* **1989**, *54*, 1766.
(10) Moutet, J.-C.; Saint-Aman, E.; Ungureanu, M.; Visan, T. *J. Electroanal. Chem*. **1996**, *410*, 79.

10.1021/ic000859h CCC: $20.00
Published on Web 05/31/2001

Chart 1

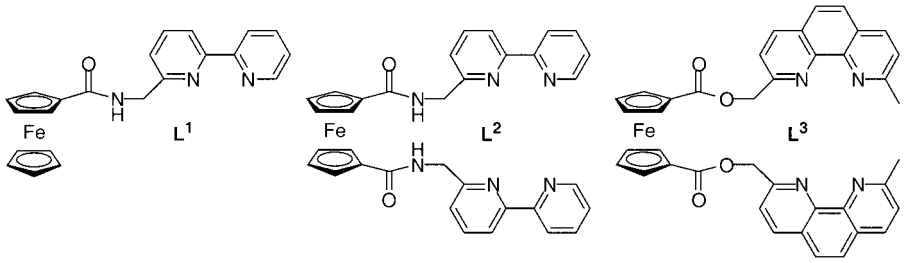

and 2H, respectively., *H*-*m*-bipy), 9.1 (4H, *H*-*p*-bipy), −8.0 (4H, C*H*$_2$-bipy), 5−0 (*H*-Cp). Anal. Calcd for $C_{44}H_{38}N_6O_{10}Fe_3Cl_2 \cdot 3H_2O.CH_2Cl_2$: C, 45.49; H, 3.90; N 7.07. Found: C, 45.25; H, 3.65; N, 7.26.

[FeL^2](ClO$_4$)$_2$. Yield, 95%. FAB$^+$-MS, *m*/*z*: 763 ([Fe**L**^{2}](ClO$_4$)$^+$; 34%), 663 ([Fe**L**^{2}]$^{2+}$ − H$^+$; 100%). UV−vis (LMCT band; CH_3CN) λ_{max} (ϵ/M^{-1} cm^{-1}) = 460 nm (830). FT-IR: ν_{CO} = 1598 cm^{-1}. ^{1}H NMR (300 MHz, CD_3CN, 10 mM, 295 K) δ: 147.5 (2H, *H*-*o*-bipy), 71.4 (2H, *H*-*o*-bipy or N*H*), 62.0 (2H, *H*-*m*-bipy), 61.2 (2H, *H*-*m*-bipy), 56.8 (2H, *H*-*m*-bipy), 48.7 (2H, *H*-*m*-bipy), 23.2 (2H, C*H*$_2$-bipy), 9.2 (2H, *H*-*p*-bipy), 3.8 (2H, *H*-*p*-bipy), −9.5 (2H, C*H*$_2$-bipy), 5−0 (4 signals, 8H, *H*-Cp). Anal. Calcd for $C_{34}H_{28}N_6O_{10}Fe_2Cl_2$: C, 47.31; H, 3.27; N, 9.74. Found: C, 46.87; H, 3.38; N, 9.68.

[FeL^3](ClO$_4$)$_2$. Yield, 94%. FAB$^+$-MS, *m*/*z*: 841 ([Fe**L**^{3}](ClO$_4$)$^+$; 91%), 742 ([Fe**L**^{3}]$^+$; 30%), 687 (**L**^{3} + H$^+$; 100%). UV−vis (LMCT band; CH_3CN) λ_{max} (ϵ/M^{-1} cm^{-1}) = 450 nm (710). FT-IR: ν_{CO} = 1665 cm^{-1}. ^{1}H NMR (300 MHz, CD_3CN, 10 mM, 295 K) δ: 61.2 (2H, H_β-phen), 56.9 (2H, H_β-phen), 27.4 (4H, C*H*$_2$-phen or C*H*$_3$-phen), 9.5 (2H, H_γ-phen), 7.2 (2H, H_δ-phen), 4.3 (2H, H_γ-phen), −4.5 (4H, C*H*$_2$-phen or C*H*$_3$-phen), −27.0 (2H, C*H*$_2$-phen or C*H*$_3$-phen), 5−0 (4 signals, 8H, *H*-Cp). Anal. Calcd for $C_{40}H_{30}N_4O_{12}Fe_2Cl_2$: C, 51.04; H, 3.21; N, 5.95. Found: C, 51.33; H, 3.20; N, 6.26.

Reagents, Instrumentation and Procedure. Acetonitrile (Rathburn, HPLC grade) was used as received. Dichloromethane was dried over neutral alumina (activity I) for at least 6 days. Tetra-*n*-butylammonium perchlorate (TBAP) was purchased from Fluka and dried under vacuum at 80 °C for 3 days. Electrochemical experiments were conducted in a conventional three-electrode cell under an argon atmosphere at 20 °C. The Ag/10 mM $AgNO_3$ + 0.1 M TBAP in CH_3CN was used as a reference electrode. The potential of the regular ferrocene/ferricinium (Fc/Fc^+) redox couple used as an internal standard was 0.07 V under our experimental conditions. ES (positive mode) mass spectra were recorded on a LCQ Ion Trap spectrometer. FAB (positive mode) mass spectra were recorded on a AEI Kratos MS 50 spectrometer fitted with an Ion Tech Ltd gun using *m*-nitrobenzyl alcohol as matrix.

Results and Discussion

When studied by cyclic voltammetry (CV) in CH_3CN and CH_2Cl_2 electrolytes, the free ligands **L**^{1}, **L**^{2}, and **L**^{3} are characterized by the regular one-electron reversible wave, corresponding to the Fc/Fc^+ redox couple.[4,8] This wave decreases upon addition of increasing amounts of Fe^{2+} as its $Fe(ClO_4)_2 \cdot 6H_2O$ salt, and it is gradually replaced by a new wave which emerges at a more positive potential (Figure 1 for **L**^{2} + Fe^{2+} for example, and Table 1). This electrochemical behavior indicates that the redox ligands are complexed by Fe^{2+} and is attributed to strong interactions between the complexed metal cation and the ferrocenyl subunit in its neutral and oxidized forms. Complexation of **L**$^{1-3}$ with Fe^{2+} also gives rise to more positive potentials in a third redox peak system attributed to the complexed Fe^{II}/Fe^{III} redox couple, discussed hereafter.

The addition of increasing amounts of Fe^{2+} to a CH_3CN solution of **L**^{1} leads first to the formation of [Fe**L**$^1_3$]$^{2+}$ species, then to the [Fe**L**$^1_2$]$^{2+}$ species, as evidenced from rotating disk electrode voltammetry (Figure 2) and CV measurements. The gradual decrease of the wave corresponding to the free Fc/Fc^+ redox couple ($E_{1/2}$ = 0.27 V; labeled I in Figure 2A, curves a, b), which fully vanished at $Fe^{2+}/$**L**^{1} = 0.5 (Figure 2A, curve c), is accompanied by the rise of new waves, labeled II, III, IV, and V (curves b−d). The amperometric titration curves recorded at different potentials are shown in Figure 2B. The redox processes II + III correspond to the electrochemical response of the complexed Fc centers in both the [Fe**L**$^1_3$]$^{2+}$ and [Fe**L**$^1_2$]$^{2+}$ species, reaching full development at $Fe^{2+}/$**L**^{1} = 0.5 (Figure 2A, curve c, and Figure 2B). An average value of $E_{1/2}$ = 0.39 V was measured for these two close redox couples, which appeared to be reversible from CV experiments (ν = 0.1 V s^{-1}). In contrast, the intensity of the reversible process IV goes through a maximum at 0.35 molar equiv of Fe^{2+} and tends toward zero at about $Fe^{II}/$**L**^{1} = 0.6 (Figure 2B). It can thus be attributed to the reversible one-electron Fe^{II}/Fe^{III} oxidation in a [Fe**L**$^1_3$]$^{2+}$ complex. Its half-wave potential ($E_{1/2}$ = 0.77 V) is close to that found for the regular [Fe(bipy)$_3$]$^{2+}$ complex ($E_{1/2}$ = 0.76 V) in CH_3CN electrolyte.[2] Adsorption of the Fe complex onto the electrode surface precluded an accurate measurement of the evolution of the wave corresponding to process V. However, the height of the RDE wave for process V in the presence of an excess of Fe^{II} (e.g. one molar equiv; Figure 2A, curve d) is half of that corresponding to the original I, indicating that two metallo-ligands are involved in the complex formed under these experimental conditions. It can thus be assumed that this wave is due to the reversible one-electron Fe^{II}/Fe^{III} oxidation in the [Fe**L**$^1_2$]$^{2+}$ complex. Its $E_{1/2}$ value (0.97 V) is close to that already attributed to a [Fe(bipy)$_2$]$^{2+}$ complex.[2,3] From CV experiments, this redox process appeared to be weakly reversible (I_{pa}/I_{pc} markedly greater than 1, at ν = 0.1 V s^{-1}). This is probably due to a decomplexation phenomena resulting from the establishment of strong repulsive electrostatic forces between Fc^+ and Fe^{III} centers in the fully oxidized complex. In

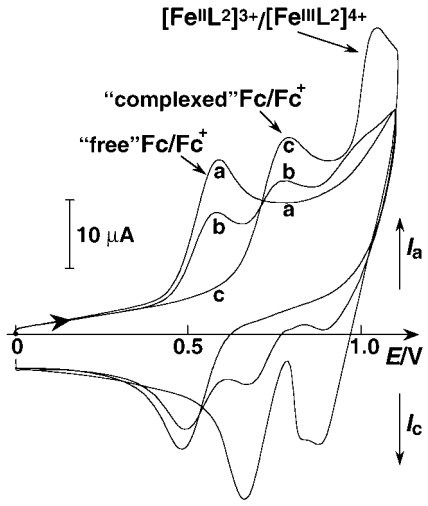

Figure 1. Cyclic voltammograms at a glassy carbon disk (5 mm diameter) of **L**^{2} (0.6 mM) in CH_3CN + TBAP 0.1 M: (a) free **L**^{2}; (b) **L**^{2} + 0.5 Fe^{2+}; (c) **L**^{2} + 1 Fe^{2+}; scan rate 0.1 V s^{-1}.

Table 1. Redox Data[a] for Ligands $\mathbf{L}^{1-3}$ and Their Iron Complexes

$\mathbf{L}^1$				L^2			L^3		
free $\mathbf{L}^1$	$\mathbf{L}^1 + Fe^{2+}$			free $\mathbf{L}^2$	$L^2 + Fe^{2+}$		free $\mathbf{L}^3$	$L^3 + Fe^{2+}$	
Fc/Fc^+	Fc/Fc^+	Fe^{II}/Fe^{III}	Fe^{II}/Fe^{III}	Fc/Fc^+	Fc/Fc^+	Fe^{II}/Fe^{III}	Fc/Fc^+	Fc/Fc^+	Fe^{II}/Fe^{III}
		$(Fe + 3\mathbf{L}^1)$	$(Fe + 2\mathbf{L}^1)$			$(Fe + \mathbf{L}^2)$			$(Fe + \mathbf{L}^3)$
0.27	0.39	0.77	0.97	0.53 0.51[b]	0.64 0.73[b]	0.99 0.95[b]	0.58	0.85	1.31[c]

[a] $E_{1/2}$, V vs $Ag/AgNO_3$ 0.01 M + CH_3CN + TBAP 0.1 M, measured by CV in CH_3CN electrolyte; $\nu = 0.1$ V s^{-1}. [b] Measured in CH_2Cl_2 electrolyte. [c] Irreversible oxidation peak.

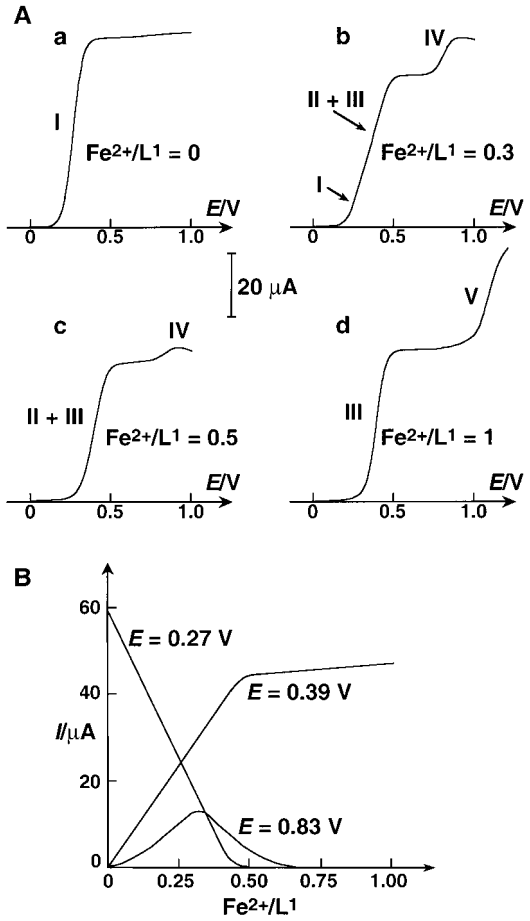

Figure 2. (A) Rotating disk electrode (Pt; 2 mm diameter) voltammetry of $\mathbf{L}^1$ (1.4 mM) in CH_3CN + TBAP 0.1 M in the presence of increasing amounts of Fe^{2+}; $\nu = 0.01$ V s^{-1}; $\omega = 600$ rev min^{-1}. (B) Variation of the oxidation current measured at three different potential values, as a function of the $Fe^{2+}/\mathbf{L}^1$ ratio.

fact, the metal centered oxidation occurs after that of the ferrocenyl unit, such as in the $[Fe^{II}\mathbf{L}^1{}_2]^{4+}$ complex.

These results have been corroborated by UV−vis experiments. Upon addition of Fe^{2+} to a CH_3CN solution of $\mathbf{L}^1$, a large bathochromic shift of the original d−d band of the free ligand at 440 nm ($\epsilon = 220$ M^{-1} cm^{-1}) is observed until ca. 0.35 molar equiv in Fe^{II} has been added. The maximal shift is about 25 nm. Further addition of Fe^{II}, up to 0.6 molar equiv, induces an hypsochromic shift (10 nm). No isosbestic point was observed on the UV−vis titration curve; this suggests that the complexation process of $\mathbf{L}^1$ with Fe^{II} involves two species at equilibrium. Correlation of the absorbance measured at 440 nm versus the concentration of Fe^{2+} presents an inflection point at $Fe^{2+}/\mathbf{L}^1 = 0.5$. This bis(bipy) complex is characterized by LMCT band at 450 nm ($\epsilon = 610$ M^{-1} cm^{-1}) overlapping the d−d band of the ferrocenyl subunit. The MLCT band for the $[Fe(bipy)_2]^{2+}$ complex in CH_3CN has been found at $\lambda = 470$ nm, while that for the $[Fe(bipy)_3]^{2+}$ complex is located at $\lambda = 521$ nm under the same experimental conditions.[2] Furthermore, the titration curves recorded at 455 and 525 nm show a maximum at $Fe^{II}/\mathbf{L}^1 = 0.35$, in agreement with the formation of an intermediate $[Fe\mathbf{L}^1{}_3]^{2+}$ complex.

The progressive complexation of $\mathbf{L}^2$ with Fe^{2+} gave simple CV features in both CH_2Cl_2 (Figure 1) and CH_3CN electrolytes. The redox system corresponding to the complexed Fc/Fc^+ couple reaches full development at $Fe^{2+}/\mathbf{L}^2 = 1$, and this is accompanied by the rise of a well-behaved pair of peaks attributed to the Fe^{II}/Fe^{III} reversible oxidation in the $[Fe\mathbf{L}^2]^{2+}$ complex (Figure 1, curve c; splitting of the reduction peak is probably due to adsorption phenomena and is not seen in CH_3CN electrolyte). Its $E_{1/2}$ value (0.99 V in CH_2Cl_2 and 0.95 V in CH_3CN) is close to that found for the $[Fe\mathbf{L}^1{}_2]^{2+}$ complex (Table 1) and is in keeping with "$Fe(bipy)_2$" complexes. It should be emphasized that no redox peaks system attributed to the intermediate formation of $[Fe(bipy)_3]^{2+}$-like species could be seen during the progressive complexation of $\mathbf{L}^2$ with Fe^{2+}. The same CV features were obtained in CH_3CN electrolyte, although the Fe^{II} centered oxidation appeared less reversible. The 1:1 stoichiometry of the $\mathbf{L}^2 + Fe^{2+}$ complex has been corroborated by UV−vis titration (LMCT band, λ_{max} (ϵ/M^{-1} cm^{-1}) = 460 nm (830); d−d band in free $\mathbf{L}^2$, λ_{max} (ϵ/M^{-1} cm^{-1}) = 440 nm (250)) and by the FAB-MS spectrum of the isolated complex (see the Experimental Section). The same MS spectrum was obtained with the complex isolated from a solution containing an excess of ligand ($\mathbf{L}^2/Fe^{2+} = 1.5$).

The crystal structure of this complex (Figure 3 and Table 2) reveals that the iron(II) coordination environment consists of four nitrogen atoms provided by the bipy subunits and two oxygen atoms of the carbonyl groups, describing a distorded octahedral arrangement. Fe2−N3 and Fe2−N23 bond distances are equal (2.148(2) Å) and shorter than both the Fe2−N2 (2.186(2) Å) and Fe2−N22 (2.194(2) Å) distances. The atoms O1, O2, N3, and N23 form a square plane around the Fe2. The N2 and N22 atoms occupy axial positions, with a N2−Fe2−N22 angle of 173.1°. The short Fe2−O1 and Fe2−O2 bonds (2.130(2) Å and 2.096(2) Å, respectively) indicate a strong coordination between the metal center and the oxygen atoms of the carbonyl groups, in agreement with the marked drop (38 cm^{-1}) in the ν_{CO} stretching vibration (1598 cm^{-1} in the Fe(II) complex, and 1636 cm^{-1} in the free ligand).[11] The "cis" and "trans" angles range from 76.1° to 99.5° and from 172.1° to 173.8°, respectively. The Cp rings remain almost coplanar relative to one another (angle of 4.7°).

This coordination is quite unexpected. For example, it has been reported that reaction of Fe^{2+} with tetradentate ligands consisting of two bipy subunits linked by a bis-amide spacer led to a helical dinuclear tris(bipy) iron(II) complex, without

(11) CO stretching bands move to lower wavenumber by ca. 30 cm^{-1} in complexed carboxylic acid amides; see: Paul, R. C.; Moudgil, A. K.; Chadha, S. L.; Vasisht, S. K. *Indian J. Chem.* **1970**, *8*, 1017.

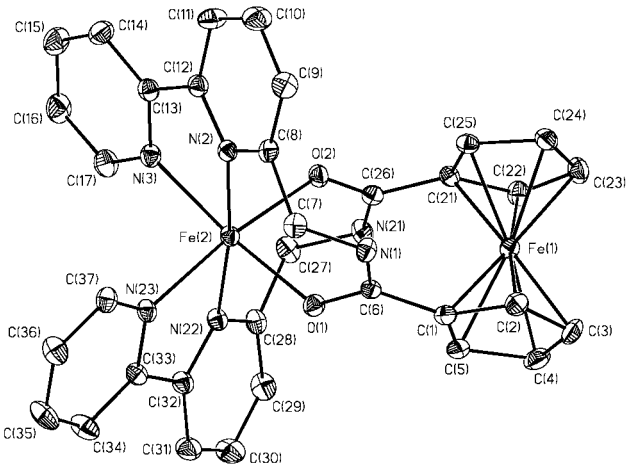

Figure 3. X-ray structure of the $[Fe\mathbf{L}^2](ClO_4)_2$ complex. Hydrogen atoms are omitted. Selected interatomic distances (Å) and angles (deg): Fe(2)−N(3), 2.148(2); Fe(2)−N(23), 2.148(2); Fe(2)−N(2), 2.186(2); Fe(2)−N(22), 2.194(2); Fe(2)−O(1), 2.130(2); Fe(2)−O(2), 2.096(2); O(1)−C(6), 1.260(3); O(2)−C(26), 1.260(3); N(1)−C(6), 1.323(3); N(21)−C(26), 1.326(3); N(2)−Fe(2)−N(22), 173.1(6); O(1)−Fe(2)−N(3), 173.7(6); O(2)−Fe(2)−N(23), 172.2(7); O(1)−Fe(2)−N(3), 173.7(6); N(23)−Fe(2)−N(2), 99.4(1); N(23)−Fe(2)−N(22), 76.2(7).

Table 2. Crystal Data and Structure Refinement for $[Fe\mathbf{L}^2](ClO_4)_2$ and $[Fe\mathbf{L}^3](ClO_4)_2$

	$[Fe\mathbf{L}^2](ClO_4)_2$	$[Fe\mathbf{L}^3](ClO_4)_2$
chemical formula	$C_{39.5}H_{40.5}Cl_2Fe_2N_6O_{14.5}$	$C_{40}H_{30}Cl_2Fe_2N_4O_{12}$
formula weight	1013.88	941.28
space group	*P*1	*C*2/*c*
T (K)	298 ± 1	298 ± 1
a (Å)	10.4175(8)	20.1487(14)
b (Å)	12.9879 (10)	15.9302 (10)
c (Å)	17.7625(14)	12.9045 (9)
α (deg.)	110.2090(10)	
β (deg.)	96.944(2)	116.5490(10)
γ (deg.)	103.643(2)	
ν (Å^3)	2137.1(3)	3705.2(4)
ρ (g cm^{-3})	1.576	1.687
Z	2	4
μ (mm^{-1})	0.880	1.002
R^a	0.0507	0.0921
$R_w{}^b$	0.0891	0.0992

$^a R = \sum||F_o| - |F_c||/\sum|Fo|$. $^b R_w = [\sum w(|F_o| - |F_c|)^2/[\sum wF_o^2]^{1/2}$.

any evidence for an $Fe^{II}-O{=}C_{amide}$ interaction,[12] despite the fact that Fe^{II}−formamide coordination through oxygen has been evidenced.[13] It is surmized that the coordination of the carbonyl moiety to the iron center in the present complex is driven by the chelating effect, which forces the carbonyl to lie in a cis conformation. Furthermore, electron density on the oxygen atom might be increased due to conjugation of the carbonyl group with the electro-releasing ferrocenyl moiety.[14] The fact that the fully oxidized complex (with the ligand in the form of the essentially innocent ferricinium) is rather stable on the CV time-scale is evidence of a strong coordination of the amide and ester (see below) moieties. In addition, electrochemical experiments have shown that the $[Fe\mathbf{L}^2]^{2+}$ complex is more stable than its parent $[Fe\mathbf{L}^1{}_2]^{2+}$ complex. Evidently, the ligand $\mathbf{L}^2$ consisting of two bipy units linked by a ferrocenyl spacer creates a favorable structural environment around the Fe^{2+} cation.

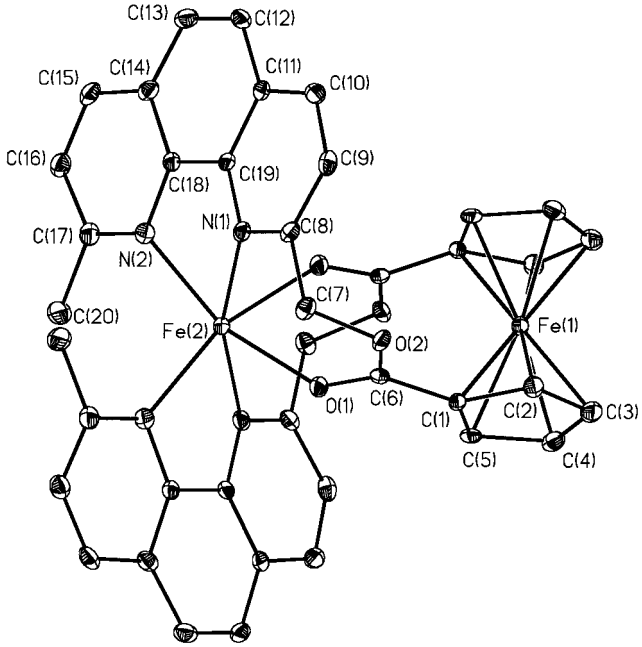

Figure 4. X-ray structure of the $[Fe\mathbf{L}^3](ClO_4)_2$ complex. Hydrogen atoms are omitted. Selected interatomic distances (Å) and angles (deg): Fe(2)−N(1), 2.208(3); Fe(2)−N(2), 2.154(3); Fe(2)−O(1), 2.164(3); O(1)−C(6), 1.229(5); O(2)−C(26), 1.330(4); N(2)−Fe(2)−O(1), 161.5(1); N(2)−Fe(2)−N(1), 76.8(1); O(1)−Fe(2)−N(1), 86.6(1).

Iron(II) also forms with $\mathbf{L}^3$ a 1:1 complex $[Fe\mathbf{L}^3]^{2+}$, as shown by the FAB-MS spectrum of the isolated complex (see the Experimental Section). The marked drop in the ν_{CO} stretching vibration (48 cm^{-1}) is consistent with coordination of Fe^{II} to the oxygen atoms of the carbonyl groups. Its crystal structure (Figure 4 and Table 2) reveals the same environment as its $[Fe\mathbf{L}^2]^{2+}$ parent complex, although the octahedral sphere is much more distorted due to the additional α-substitution of the phen subunits with methyl groups. The Fe2−N bond distances in both the square plane (2.154(3) Å) and axial positions (2.208(3) Å) are longer than in its analogue $[Fe\mathbf{L}^2]^{2+}$; this is due to the steric crowding of the methyl substituents. The "cis" angles around Fe2 show a large variation from 76.8° to 114.6°, while "trans" angles range from 161.5° to162.0°. No significant deformation in the almost parallel Cp rings is observed (angle of 1.1°). In contrast to what is found in the $[Fe\mathbf{L}^2]^{2+}$ complex, the Fe−O distances (2.164(3) Å) are longer than the Fe−N distances, indicating a weaker bonding of the iron center to carbonyl oxygen atoms of the carboxy-ester groups. This point has been confirmed by CV experiments carried out with the isolated complex (Table 1). Oxidation of the ferrocene center in the complex leads to its partial decomplexation, as shown by the appearance on the reverse scan of the Fc/Fc^+ peak system corresponding to the free ligand. Furthermore, oxidation of the iron(II) center occurs at a high potential (1.31 V) and is fully irreversible.

The ^{1}H NMR spectra of $[Fe\mathbf{L}^1{}_2]^{2+}$, $[Fe\mathbf{L}^2]^{2+}$, and $[Fe\mathbf{L}^3]^{2+}$ were tentatively assigned after comparison of the spectra of the three complexes and correlations observed in 2D COSY GP experiments in the case of $[Fe\mathbf{L}^2]^{2+}$ and $[Fe\mathbf{L}^3]^{2+}$ (see the Experimental Section). These spectra displayed resonances ranging from 70 to −8 ppm, 140 to −10 ppm, and 60 to −30 ppm, respectively, attesting to a high spin configuration for the three complexes. The ^{1}H NMR spectrum of $[Fe\mathbf{L}^1{}_2]^{2+}$ displays broad peaks due to a rapid exchange on the NMR time scale of the two $\mathbf{L}^1$ ligands in the iron coordination sphere, preventing a 2D COSY GP experiment. It should be pointed out that such

(12) Baret, P.; Gaude, D.; Gelon, G.; Pierre, J.-L. *New J. Chem.* **1997**, *21*, 1255.
(13) Constant, G.; Daran, J.-C.; Jeannin, Y. *J. Inorg. Nucl. Chem.* **1971**, *33*, 4209.
(14) Nesmeyanov, A. N.; Perevalova, E. G.; Gubin, S. P. *Tetrahedron Lett.* **1966**, *22*, 2381.

a high spin configuration differs from the low spin (S = 0) configuration of the $[Fe(bipy)_2(CH_3CN)_2](ClO_4)_2$ complex.[2,3] The presence of oxygen atoms from the amide or ester groups leads to a lower ligand field than results from the nitrogen atoms from acetonitrile. This is confirmed by the UV−vis data, which show that the molar extinction coefficient of the visible transition is lower in $[Fe\mathbf{L}^1{}_2]^{2+}$, $[Fe\mathbf{L}^2]^{2+}$, and $[Fe\mathbf{L}^3]^{2+}$ (see the Experimental Section) than in $[Fe(bipy)_2(CH_3CN)_2](ClO_4)_2$ ($\epsilon = 5600$ M^{-1} cm^{-1} at 470 nm).[2]

Further studies will be directed toward the use of these novel complexes in catalytic oxidations.

Acknowledgment. The authors thank Region Rhône-Alpes for partial financial support through the TEMPRA Program. We are grateful to Dr Alain Deronzier and Dr Jean-Claude Lepretre for fruitful discussions.

Supporting Information Available: X-ray crystallographic files in CIF format for the structure determinations of $[Fe\mathbf{L}^2](ClO_4)_2$ and $[Fe\mathbf{L}^3](ClO_4)_2$. This material is avaible free of charge via the Internet at http://pubs.acs.org.

IC000859H